Sticky bubbles

Océ

Sticky Bubbles

Oleg Antoniuk[1], Arjan van de Bos[2], Theo Driessen[3], Bram van Es[4]
Roger Jeurissen[5], Dominik Michler[1], Hans Reinten[2], Marieke Schenker[6]
Jacco Snoeijer[3], Sudhir Srivastava[5]
Federico Toschi[5] & Herman Wijshoff[2]

[1] *University of Amsterdam, the Netherlands*
[2] *Océ, the Netherlands*
[3] *University of Twente, the Netherlands*
[4] *Rijnhuizen, the Netherlands*
[5] *Eindhoven University of Technology, the Netherlands*
[6] *Delft University of Technology, the Netherlands*

Abstract

We discuss the physical forces that are required to remove an air bubble immersed in a liquid from a corner. This is relevant for inkjet printing technology, as the presence of air bubbles in the channels of a printhead perturbs the jetting of droplets. A simple strategy to remove the bubble is to flush the ink past the bubble by providing a high pressure pulse. In this report we first compute the viscous drag forces that such a flow exerts on the bubble. Then, we compare this to the "sticking forces" on the bubble, due to the capillary interaction with the wall. From this we can estimate the required flow velocities for bubble removal, as a function of channel geometry, contact angle and ink properties. Finally, we investigate other ways to exert a force on a trapped bubble. In particular we focus on forces induced by electric fields which can alter the contact angle of the drop, or by locally applying thermal gradients. Once again, these forces are compared to the sticking forces to identify the parameters where the bubble can be removed.

1 Company profile

Océ is a global leader in digital document management and delivery technology offering software solutions. Océ makes a wide range of imaging equipment. Its products include digital copiers, printers, scanners, imaging systems and related supplies for the office, printing, and engineering markets. At our own R&D locations worldwide, Océ products are invented and engineered. The largest R&D site is in Venlo with about 800 employees, mostly highly educated engineers in physics, mechanics, electronics, chemistry, information technology and industrial design. In our Venlo R&D inkjet is a fast-growing core technology.

2 Problem description

In many inkjet systems air bubble entrapment in one of the ink channels sometimes occurs resulting in nozzle failure and poor print quality. There are several methods to prevent or to solve this event. One way of prevention is ink circulation in the print head. The ink flow will then remove the air bubble away from the ink chamber and the jetting process will not be disturbed. One way of solving is to flush the microfluidic system using a pressure pulse at the entrance.

The general problem of air bubble removal applies to different embodiments and geometries used by Océ and several other companies. In order to optimize designs now in development and for next developments Océ wants to have a better understanding of the basic physics involved and get quantitative data on thresholds for removal of bubbles. However the implementation of the ink circulation requires a thorough modeling of the ink flow. The problems below address parts of the total problem. However basic, these cases require a knowledge of fluid mechanics and seems to be challenging enough to keep a group of student busy for several days.

1 An air bubble is created in the angle of the L-shape tube with rectangle cross-section filled with a liquid (see left hand side of figure 1). Calculate the minimum air bubble diameter and minimum liquid velocity necessary for transferring the bubble out of the corner. Consider several cases for bubble contact angle and liquid type. The flow through the system should remain laminar. Consider the tube surface as perfectly flat.

2 An air bubble is created in a fluid chamber located between a filter and a narrow fluid passage (see right hand side of figure 1). By applying a pressure pulse (time, amplitude) on the fluid above the filter fluid will be pushed through the passage and may entrain the bubble into the passage. Fluid flow amplitude will depend on pressure and viscous resistance of the passage itself and the fluid system after the passage. This total resistance i.e. pressure needed to create the flow is a parameter to be considered. The pressure will deform the bubble. Determine the parameter space of pressure and volume flow (amplitude, time), bubble (size), material properties (fluid viscosity and surface tension, contact angles) and geometry (angle of the corner, diameter of the passage, size of the chamber) for which the bubble will or will not be entrained into the passage. Dimensions given are indicative.

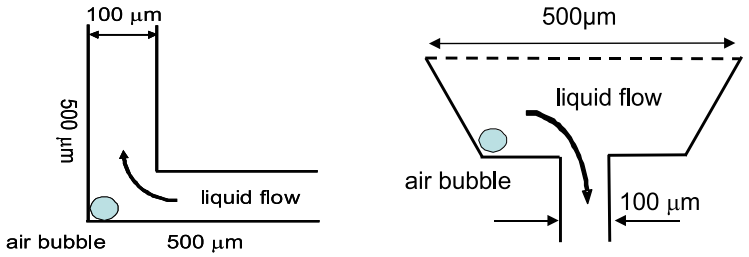

Figure 1: A schematic view of the two problems

3 Problem solving strategy

The goal of the project is to investigate how air bubbles can be removed from a corner. The main origin of the problem is that the acoustic (pressure) fields during jetting induce a force that naturally drives bubbles to the wall, and preferably into corners. The currently employed strategy is to remove the bubbles by flushing (or purging) the ink channels once the acoustic field is switched off. In this research we focus on the forces needed to remove the bubbles and aim to reveal the basic flushing dynamics in the vicinity of the corner. For this we address the following questions:

- What is the flow field in the vicinity of a corner? In particular, is there a zone of recirculation that could impede the flushing of a bubble?
- Is the bubble in direct contact with a wall or is separated from the wall by a thin film of ink?
- What are the forces and flow velocities required to remove a bubble from a corner?
- Are there other ways to exert forces on a bubble, as an alternative to flushing?

We first discuss basic features of the flow field in the whole printerhead and near a corner, both with and without the presence of an acoustic field (see chapter 4. We consider the situation when a bubble is present without touching the wall. The hydrodynamic forces on the bubble are estimated in chapter 5 and we derive the timescales relevant for the flushing process (see chapter 5.3). Chapter 6 discusses the case where the bubble is in contact with the wall. We compute the surface energy of the bubble inside and outside the corner, from which we can estimate the force required to remove the bubble. This is then compared to the viscous drag that can be achieved by flushing. In chapter 7 we explore alternative ways to force a bubble. In particular we consider capillary forces induced by thermal gradients and electrostatic interactions. Our results leads to a set of conclusions and recommendations for Océ, which are summarized in chapter 8.

4 Flow regimes

This chapter describes the two flow regimes that occur within the printerhead. First the flow occurring during normal operation is characterized. Section 4.2 treatens the flow occurring during the flushing of the head. In both cases the presence of bubbles has not been accounted for.

4.1 During jetting

When droplets are being jetted, the flow in the channel is characterized by two dimensionless groups. To determine these dimensionless groups, the following parameters of the flow are used.

$$\begin{aligned} u_c &= 0.6\ ms^{-1} \quad \text{maximum velocity in the channel} \\ \omega &= 250\ kHz \quad \text{angular frequency of oscillatory flow} \\ \eta &= 0.01\ Pa\,s \quad \text{viscosity} \\ \gamma &= 0.03Nm^{-1} \quad \text{density} \\ R_c &= 125\ \mu m \quad \text{channel radius} \end{aligned} \tag{1}$$

The first dimensionless group is the Reynolds number.

$$\mathrm{Re} = \frac{uR_c\rho}{\eta} \sim 0.1 \tag{2}$$

The Reynolds number is the ratio of steady inertia over viscosity. The small value indicates that fr the steady component of the flow, inertia can be neglected. The second dimensionless group is the Womersley number.

$$\mathrm{Wo} = \sqrt{\frac{\omega R_c^2\rho}{\eta}} = 21 \tag{3}$$

The Womersley number is the ratio of unsteady inertia over viscosity. The large value indicates that the viscous boundary layer is thin. This is helpful for removal of the bubble.

4.2 During flushing

If the printheads are flushed/purged a large pressure gradient is imposed over a relatively long time period (in the order of 1 second) and the ink is pushed out of the head. Flushing is one of the possible means to remove air bubbles in the ink. Flushing can be considered as a continuously applied pressure gradient over the head during some time period. The ink in the head will move from the inlet to the nozzle. To get some idea of the average velocity due to the pressure gradient we use the Hagen-Poiseuille equation for the channel

$$\Delta p = \frac{8\eta L u}{R^2}, \tag{4}$$

using channel radius $R = 125\mu m$, $L = 400\mu m$ with a pressure gradient of $10kPa$ gives a mean channel velocity of about 5 m/s, which seems very large. If we simulate this with a Navier-Stokes solver (see Jeurissen (2009)), including the nozzle which has a radius of $30\mu m$ and a height of $50\mu m$ we get $u_{mean} \approx 1$ m/s in the nozzle, see figure 2.

The average flow velocity in the nozzle and in the channel will be different primarily because of the different areas of the nozzle and the flow channels. Since the mass flow rate in the channel and the nozzle should be equal the following holds:

$$\rho\, u_{channel} A_{channel} = \rho\, u_{nozzle} A_{nozzle}, \tag{5}$$

which results in $u_{avg,channel} = (15/125)^2$, $u_{avg,nozzle} \approx 0.0144$m/s. For the Reynolds number we use different length scales for the channel and for the nozzle.

$$Re_{channel} = \frac{\rho L u}{\eta} \approx \frac{1090\, 250 \exp(-6)\, 0.0144}{0.01} = 0.4, \quad Re_{nozzle} = \frac{1090\, 15 \exp(-6)\, 1}{0.01} = 1.635, \tag{6}$$

Looking at the streamlines the entire flow seems to be laminar, therefore we assume we are dealing with a Stokes flow, see figure 3. For the flush case, with the time continuous pressure gradient we can assume that the Stokes flow is steady.

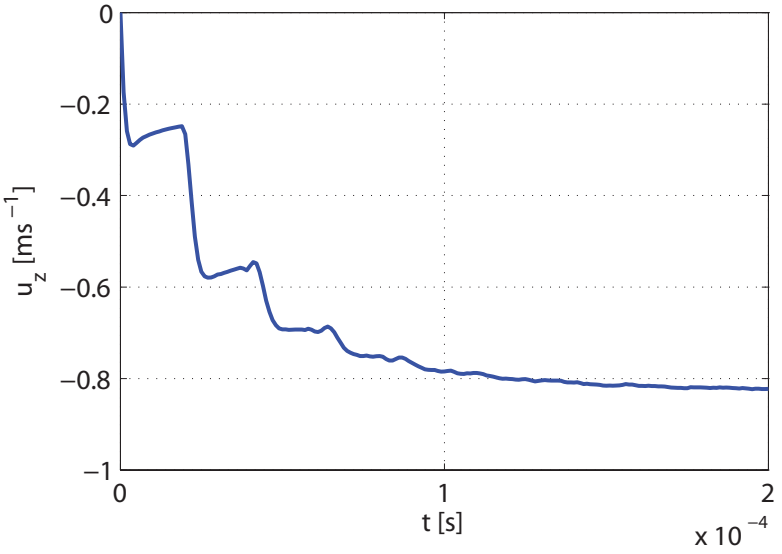

Figure 2: Mean nozzle velocity after 10 kPa flush

4.3 Viscuous eddies

Stokes flow near a sharp corner induces viscous eddies. A similarity solution for these eddies has been found by Moffatt (1964). The streamlines inside the Moffatt eddies are closed, hence the flushing of a bubble can be hindered by the existence of Moffatt eddies. A schematic example of the Moffatt eddies is shown in figure 4.

From the similarity solution the ratio of the successive distances of the centers can be found by:

$$\frac{r_i}{r_{i+1}} = e^{\pi/q_i} \tag{7}$$

where r is the distance between the eddie and the sharp edge and q_i is the imaginary part of the eigenvalue of the similarity solution. For the case of an angle of 90°, the imaginary part of the eigenvalue is 0.6 (Moffatt (1964)). This leads to a ratio in the distances of 500. Since the maximum size of an eddie inside the ink chamber is the size of the chamber itself: around 200 micrometer, the next eddie can be expected under 1 micrometer distance from the corner. This is way below the critical bubble radius, hence a bubble of this size would immediately dissolve into the ink.

5 Forces on a detached bubble

The forces on a bubble detached from the surface are evaluated. First the force that drives the bubble towards the corner is explained. The forces that are exerted on the bubble during flushing are estimated in section 5.2.

5.1 During jetting

Two acoustic forces act on the bubble during normal printing. These forces are the primary Bjerknes force and the secondary Bjerknes force. The first is the buoyant force on the bubble due to the acoustic field. The second is the buoyant force on the bubble due to the pressure gradient that is caused by the volume oscillations of the bubble. Primary Bjerknes force is not considered here. A more detailed treatment may be found in Jeurissen (2009). The secondary Bjerknes force F_{sec} is the force that traps the bubble in the corner. It would vanish for a bubble in an infinite volume of liquid, but it is nonzero due to the presence of the channel walls and the meniscus at the nozzle. Secondary Bjerknes force pushes bubbles away from free surfaces and towards walls. The magnitude of this force depends on the bubble volume. Under normal operating conditions, the ratio of drag over secondary Bjerknes force is large for bubbles that are smaller than $R_b = 10\ \mu m$, unless the bubble is

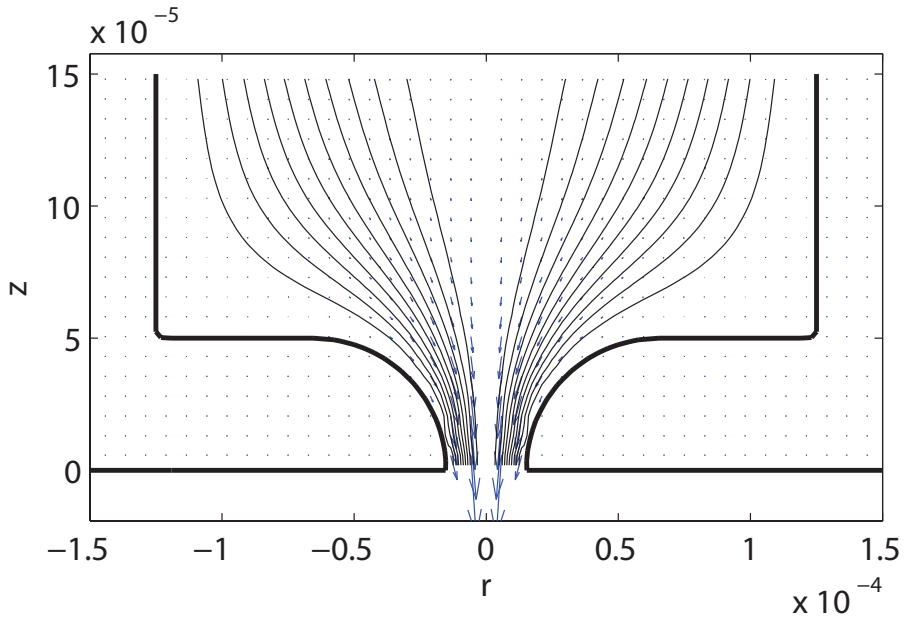

Figure 3: Streamlines for the flush case

very close to the wall.

$$\frac{F_d}{F_{\text{sec}}} = \frac{9\eta u R_c}{4\pi\rho\omega^2 R_b^5} \tag{8}$$

The distance to the wall has been taken to be equal to the channel radius. The ratio of these forces is proportional to the fifth power of the bubble radius, which is rather steep. Therefore, secondary Bjerknes force is dominant for bubbles larger than $R_b = 10\ \mu m$.

Secondary Bjerknes force pushes bubbles towards the walls. In the corner, there are two walls nearby. The result is that bubbles are especially attracted to corners. Since this force is dominant for all but the smallest bubbles, the bubble can only be removed from the corner when the actuation has stopped.

5.2 During flushing

The drag over a bubble in a Stokes flow is given by

$$F = 4\pi u \eta R, \tag{9}$$

which is obviously valid as long the assumptions for the Stokes flow are valid, i.e. laminar flow, incompressibility, $Re \ll 1$. Now, assuming the sphere is small and does not the influence the flow significantly we can use this simple expression for the drag estimate in the following way: suppose we have the velocity distribution of the flow in the channel, then, assuming the sphere radius is small compared to the boundary layer thickness we can use this expression to determine the sphere drag at each point of the distribution.

$$F = 4\pi u(r) \eta R, \tag{10}$$

which obviously loses validity in case the bubble size becomes of the same order as the channel width.

5.3 Flushing time

Flushing a bubble past a corner takes time. This time can be estimated by estimating the liquid velocity at the bubble and choosing at what distance the bubble is considered to be close to the corner. For the estimate of the liquid velocity, a Poiseuille flow profile is used. The distance of the bubble to the wall is taken to be equal

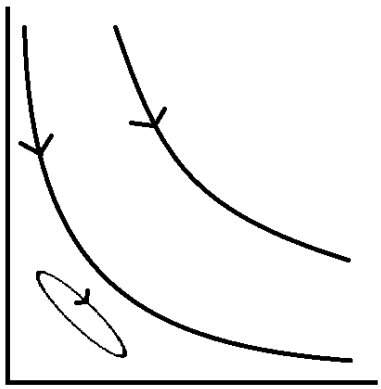

Figure 4: Sketch of a Moffat eddie in a sharp 90° corner. Since the ratio between the distances of successive vortices is 500, only one complete eddie has been drawn. In the corner we expect very small eddies, and far away we expect a large eddie.

to the bubble radius. With a Poiseuille profile, the velocity at the bubble center is nearly proportional to the bubble radius.

$$u_b = u_c \frac{2R_b}{R_c} \tag{11}$$

When the bubble is in the corner, the velocity will be lower. To take this lowering of the velocity near the corner into account, the velocity is halved. The bubble is considered to be close to the corner when the distance is smaller than the channel radius. Therefore, dividing the channel radius by the bubble velocity gives the traversal time.

$$T = \frac{R_c^2}{u_c R_b} = 0.1 \ s \tag{12}$$

The bubble radius of 15 μm was used here. This time is much shorter than the normal flushing time of 1 s. Therefore, when the actuation has been halted, removing the bubble is not a problem once the bubble has been dislodged from the corner.

6 Sticking bubble

The mobility of an air bubble on a flat surface is higher than of one trapped within a corner and is therefore better to remove from the inside of an inkjet print head. Regarding this fact, the question arises, how much work has to be delivered for a transition between these two states. We present a two dimensional analysis of this problem, by comparing the energy of these two states for different equilibrium contact angles θ and corner angles δ. From this we estimate the force to remove the bubble from the corner and compare this to viscous drag.

6.1 2D model

Within the 2D model the liquid air interface is represented as circular arc of curvature radius R, intersecting the walls of the corner with the contact angle θ with respect to the air phase, as shown in figure 5. The corner is assumed to be horizontal with one side. In order to characterize the corner, we introduce the corner angle δ, between the non horizontal wall and the horizontal. The bubble then covers a length l on both walls. The volume of the bubble is considered equivalent to the cross section area

$$A = R^2\phi - R^\circ \sin\phi\cos\phi + kR\sin\phi, \tag{13}$$

where

$$k = \sin\frac{\delta}{2} l. \tag{14}$$

and

$$\phi = \theta - \frac{\delta}{2}, \tag{15}$$

as denoted in figure 5.

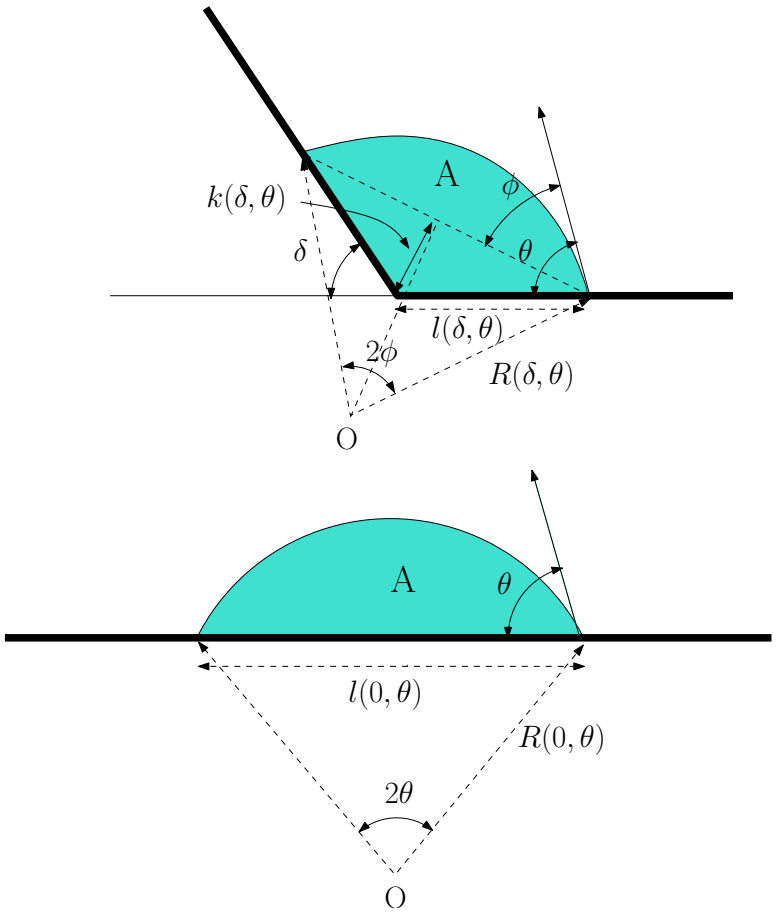

Figure 5: Sketch of the two dimensional model, showing the quantities, mentioned in the text above.

The touching length of the bubble can then be described by

$$l = R\frac{\sin\phi}{\cos\frac{\delta}{2}}. \tag{16}$$

The interfacial energy of the bubble writes as a combination of the partition from the liquid/air and the liquid/solid interface as

$$E = \gamma 2\phi R - (\gamma_{ls} - \gamma_{sv})2l. \tag{17}$$

Expression 17 can be simplified by including the Young Laplace equation

$$\gamma\cos\theta = \gamma_{ls} - \gamma_{sv}. \tag{18}$$

to

$$E = \gamma(2\phi R - 2l). \tag{19}$$

The assumption of a constant volume allows to replace the curvature radius by

$$R = \sqrt{\frac{A}{\phi - \sin\phi\cos\phi + \tan\frac{\delta}{2}\sin^2\phi}}. \tag{20}$$

With equation 15, 16 and 20 the interfacial energy can be written as a function of just four quantities, that can be measured and controlled within an potential experiment.

$$E = f(\theta, \delta, A, \gamma). \tag{21}$$

6.2 Results

In our calculations we compared the energy state of a bubble ($0° < \theta < 180°$) within a corner ($0° < \delta < 180°$) with those of a bubble of the same volume A sitting upon a flat surface

$$\Delta E = E(\theta, \delta, A, \gamma) - E(\theta, 0, A, \gamma). \tag{22}$$

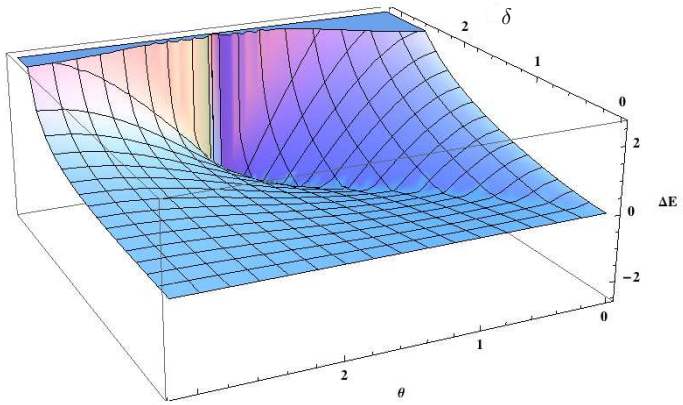

Figure 6: Energy difference landscape $\Delta E = E(\theta, \delta, 1, 1) - E(\theta, 0, 1, 1)$. The valley occurs for a liquid/air interface with no curvature along $\theta = \frac{\delta}{2}$. Partially negative values are obtained, which denotes a bubble prefers to stay in the corner.

If $\Delta E > 0$, the flat surface is preferred if $\Delta E < 0$, the corner is the preferred state for the bubble. This consideration does not take into account the states during transition from one state to the other, but only the equilibrium static energy states. Therefore it cannot give a solid statement on what will be observed in an experiment, but it provides a good estimate of energies and the forces required to remove the bubble from the corner.

Furthermore we can distinguish three wetting morphologies of the air bubble within the corner, dependent on the combination of the contact angle θ and the corner angle δ, just by geometrical considerations. By doing so, we find below a contact angle of

$$\theta_0 = \frac{\delta}{2} \tag{23}$$

an air wedge with a negative Laplace pressure (W-), which has no droplet shape, but is elongated along the entire corner. In the region of higher contact angles, positive Laplace pressure leads to an instability of this elongated structure, causing it to decay into located droplets (D+). Above a certain contact angle

$$\theta_w = \Pi - \frac{\delta}{2}, \tag{24}$$

the bubble stops to fill the entire corner and eventually the tip of the corner is filled with a liquid wedge (D+/W).

Figure 7 shows the parameter space of θ and δ, in which the combination of the energy difference ΔE and the occurrence of the three different morphologies, creates five different scenarios, which are illustrated beside the phase diagram. Thereby different scenarios for a same type of morphology are found, for different θ. For small θ the morphology (W-) is subject to scenario (A) thus has its favorable state in a plane surface and for higher θ to scenario (B) thus prefers to stay in the corner (preferred states are denoted by arrows within the sketches). For morphology (D+) the lower energy state is within the corner (C). For (D+/W) again two different scenarios (D) and (E) occur at small and higher θ respectively. Again, this scenarios only show, what the our

simple calculations deliver and should not be taken as a prediction for an experiment. The transition from one energy state to another is not linear and so probably an energy barrier has to be overcome. The most doubtful scenario is (A), since a negative Laplace pressure would oppose a detachment as shown by Prakash *et al.* (2008).

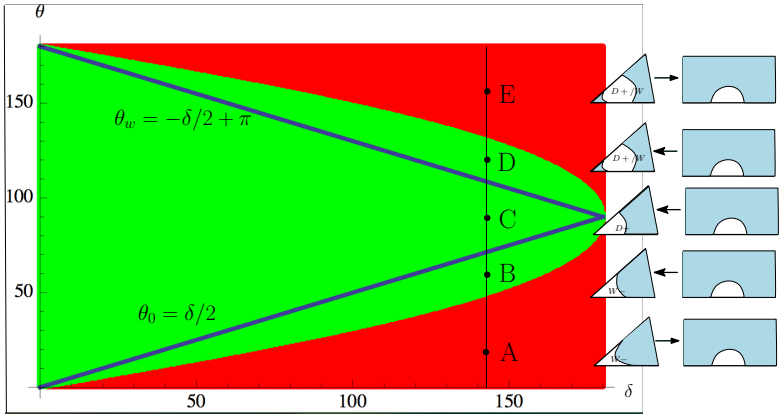

Figure 7: Phase diagram of the a bubble in a corner, showing states $\Delta E > 0$ for which the flat surface is favorable (red) and $\Delta E < 0$ for which the corner is favorable (green). The separation line $\theta_0 = \frac{\delta}{2}$ indicates vanishing Laplace pressure and $\theta_w = \Pi - \frac{\delta}{2}$. The combination of both considerations divides the diagram into five sections, within those different scenarios are shown for the corner angle $\delta = 150°$. The scenarios sketch which transition is favorable for individual morphologies for different contact angles θ.

Again, this scenarios only show, what the our simple calculations deliver and should not be taken as a prediction for an experiment. The transition from one energy state to another is not linear and so probably an energy barrier has to be overcome. The most doubtful scenario is (A), since a negative Laplace pressure would oppose a detachment as shown by Prakash *et al.* (2008). The found morphologies however are in very well agreement with Brinkmann & Blossey (2004).

6.3 3D model

A bubble can be trapped in the corner due to its surface energy. The amount of energy needed to move the bubble away from the corner can be found by comparing the change in surface areas. When one divides this energy by the distance the bubble needs to travel away from the corner, the minimal displacement force is found. This force can be used to find the minimal flushing velocity for a trapped bubble in a given corner. Due to the fact that the volume of the bubble is finite, and the fact that the contact angle is usually not exactly 90°, it is necessary to consider the energy balances of 3D bubbles, even for a 2D corner.

6.3.1 3 dimensional bubble with a contact angle of 90°

For the case of a 90 degree contact angle, only the gas-liquid interface adds to the surface energy. The energy needed to move a bubble away from a 90 degree corner is given by: The Volume is constant and given by V, the surface tension is given by γ, the energy of the corner bubble is given by E_c,energy of the bubble on a flat plate is given by E_p. The radius of the corner bubble is given by R_c, the radius of the bubble on the flat plate is given by R_p We start by taking a reference sphere of radius R, which sets the constant volume: $V = \frac{4}{3}\pi R^3$. The radius of the bubble at the edge is given by:

$$R_p^3 = 2R^3 \quad so: \quad R_p = 2^{1/3}R \tag{25}$$

$$R_c^3 = 4R^3 \quad so: \quad R_c = 4^{1/3}R \tag{26}$$

hence:

$$A_p = 2\pi R_p^2 v \quad = \quad 2^{5/3}\pi R^2 \tag{27}$$

$$A_c = \pi R_c^2 \quad = \quad 4^{2/3}\pi R^2 \tag{28}$$

The minimal energy needed to remove the bubble from the straight edge is given by:

$$\Delta E = E_p - E_c = \gamma\pi R^2(2^{\frac{5}{3}} - 4^{\frac{2}{3}}) \approx 0.65\gamma\pi R^2 \tag{29}$$

The minimal force needed to move the droplet from the 90° corner is then given by $F_\gamma = \frac{\Delta E}{R} = 0.65\gamma\pi R$. By giving a ratio between the surface tension force and the drag force on the bubble, we can find the minimal velocity necessary to remove the bubble from a straight edge. The stokes drag on a bubble is given by $F_\eta = 4\pi\eta R$.

$$\frac{R_\gamma}{R_\eta} \approx \frac{0.1\gamma}{\eta u} \tag{30}$$

When this ratio crosses 1, the viscous force exceeds the force necessary to draw the bubble from the corner, giving the critical velocity:

$$u = \frac{\gamma}{10\eta} = 0.5[ms^{-1}] \tag{31}$$

for $\gamma = 0.05\ N/m$, and $\eta = 0.01\ Pa \cdot s$.

6.3.2 3 dimensional bubble at a 90 degree edge with a contact angle below 45°

A bubble on an edge with a contact angle below $\Theta = 45°$ will show a spherical shape. Therefore bubble will have two circular contact lines with the wall, and the change of area can be found as a function of the initial volume and the contact angle. Multiplying the change in solid-liquid, solid-vapor and liquid vapor interfaces with their respective surface tensions, the change in surface energy is found. The minimal displacement distance to loose contact with one of the walls is the thickness of the red spherical caps (h) in figure 8. Hence the minimal force to detach the bubble from the wall is given by $\frac{\Delta E}{h}$. From the balance with the drag force, the minimal velocity necessary to flush the bubble is given by:

$$u = \frac{\frac{\Delta E}{h}}{4\pi\eta R_c} \tag{32}$$

The angle dependent minimal flushing velocity is shown in figure 9

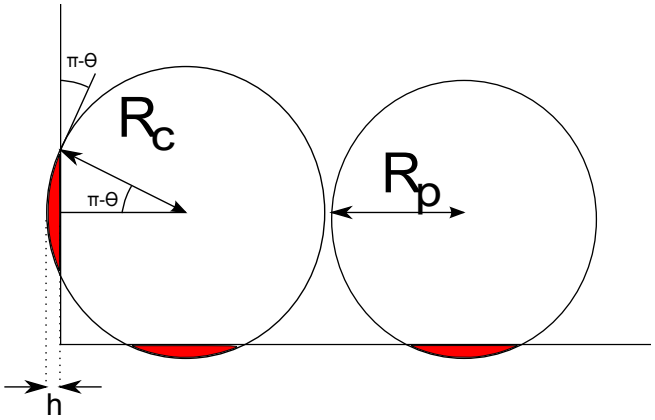

Figure 8: Removing a bubble from a partial wetting ($\Theta < 45°$) corner.

6.4 Wrap-up

Both a two-dimensional calculation and a three-dimensional calculation of the sticking force were performed. The two-dimensional calculation is relevant for large contact angles, where the bubble aspect ratio is large. In this case, the sticking force is very large. The bubble can not be flushed out in this case. However, a regime of contact angles and wedge angles has been found, where the bubble leaves the corner spontaneously.

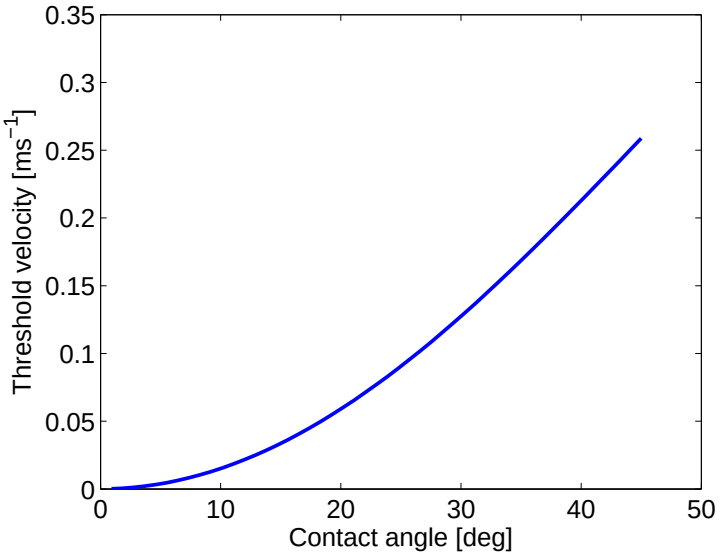

Figure 9: Velocity necessary near the bubble to remove it from the 90° edge for the given contact angle.

For small contact angles, a three-dimensional calculation revealed the dependence of sticking force on the contact angle for a wedge angle of 90°. This calculation can be extended to arbitrary wedge angles, but this was not pursued here. When the contact angle increases, the sticking force decreases monotonously to zero. In the perfect wetting case, the bubble does not stick. For a contact angle of 90°, the sticking force was calculated analytically. An ink velocity of $u = 0.5\ ms^{-1}$ at the bubble is required in this case. Since the velocity at the bubble is about a tenth of the mean velocity in the channel, and the velocity in the nozzle is 100 times as large as the velocity in the channel, the ink would be ejected from the nozzle at a velocity of 500 ms^{-1}, which requires a pressure of $P > 100\ MPa$, which is unfeasible.

7 Alternative removal mechanisms

In addition to the normal flushing operation to remove bubbles from the printhead it would be favorable to have additional mechanisms that are able to remove the bubble. A mechanism that could remove bubbles during printhead operation would be ideal, but also mechanisms removing bubble during stand still would be favorable with respect to flushing, which gives rise to the spilling of large amounts of ink.

7.1 Marangoni effect

A possible mechanism for the disposal of the bubble is thermal migration. A temperature gradient over the bubble causes a non-uniform surface tension over the surface. This gradient in surface tension induces is balanced by a motion along the surface and implies a boundary condition on the flow in the matrix liquid, the so-called Marangoni effect (Young *et al.* (1959)). A flow inside the bubble is generated as well, but due to the large ratio's between the viscosities of the bubble and matrix fluid the influence of this flow on the outer flow is negligible. A sketch of the resulting flow field with respect to the bubble is given in figure 10.

A first step in deriving the induced flow, and thus the force exerted on the bubble is the estimation of the order of magnitude of the flow for a bubble in an infinite medium. The force induced by the surface tension gradient over the bubble equals equation 33, with z the coordinate in the direction of the temperature gradient:

$$F_{th} = \int_{A_b} \frac{d\gamma}{dz} dA \tag{33}$$

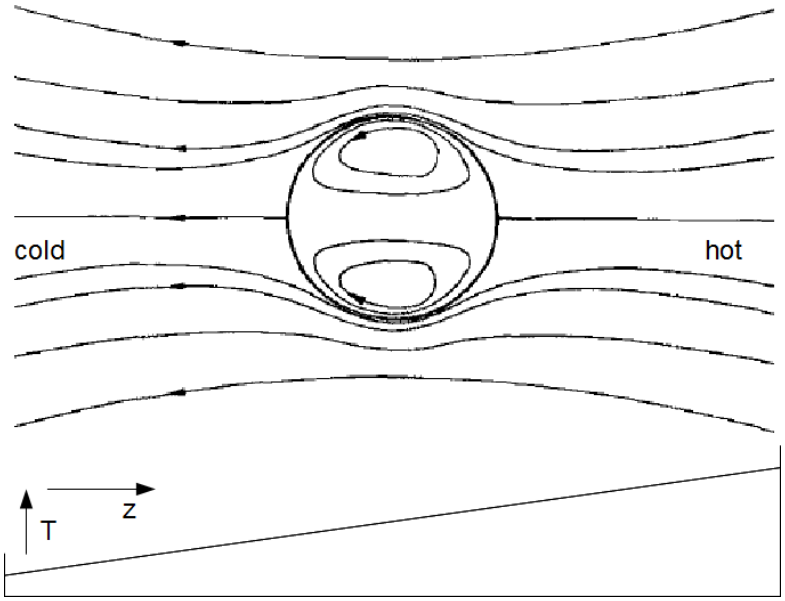

Figure 10: The flow field around a bubble in an infinite medium as induced by a thermal gradient

Which can be simplified to equation 34 to derive the order of magnitude:

$$F_{th} \approx \frac{d\gamma}{dz} A_b \tag{34}$$

The gradient in surface tension with respect to z can be obtained from the applied temperature gradient:

$$\frac{d\gamma}{dz} = \frac{d\gamma}{dT}\frac{dT}{dz} \tag{35}$$

The velocity induced by this force can be obtained using the formula for stokes drag:

$$F_D = 4\pi\eta R u \tag{36}$$

The velocity has thus a linear dependence with both bubble radius and thermal gradient. For a typical bubble observed in an inkjet-device ($R_b = 15\mu m$, liquid properties those of water) and a temperature gradient of 100 K/m, this would result in a bubble velocity of 3 mm/s.

Young *et al.* (1959) derived the terminal velocity of such a bubble for the case when both Reynolds number and Marangoni number are approaching zero, which is a reasonable good approximation for the current parameters. When gravity is neglected (we consider horizontal temperature gradients here) this equation is:

$$V_y = -\frac{2\|\frac{dT}{dz}\|\frac{d\gamma}{dT}R}{\eta(2+3\alpha)(2+\beta)} \tag{37}$$

Here α and β are the ratio's of the bubble-phase and the continuous phase for the viscosity and thermal conductivities respectively. For a gas bubble in a liquid both are negligibly small. For a water-air interface the surface tension varies linear with temperature. Figure 11 shows the obtained velocities as a function of the temperature gradient at different bubble radii.

The thermal gradient in the liquid also induces a density driven flow in the direction opposite to the induced bubble velocity. A dimensional analysis shows us that this force is negligible with respect to the thermal bubble migration at these flow conditions.

For thermal driven bubble migration to be effective as a mechanism for removing bubbles from the inkjet head, the force must be large enough to counter the forces driving the bubble towards the corner of the channel. The crucial force to withstand is the secondary Bjerknes force induced by the acoustic oscillations (see section 5.1).

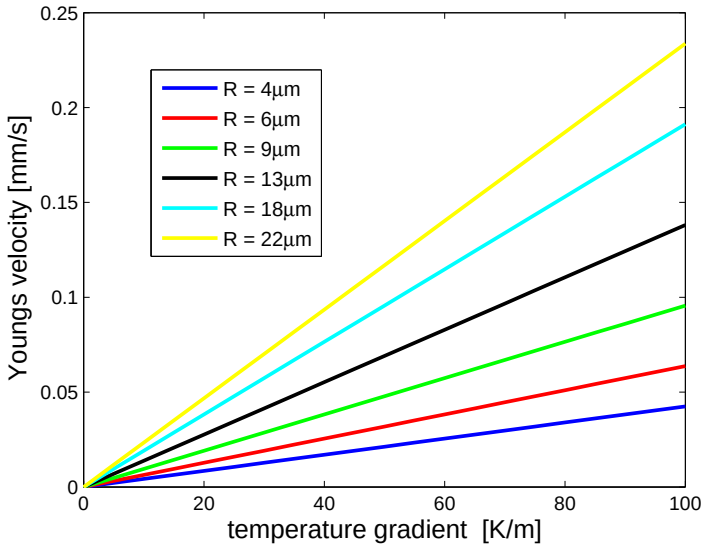

Figure 11: The flow field around a bubble in an infinite medium as induced by a thermal gradient

7.2 Bubble velocity due to the vapor transfer across the bubble

It is shown in Speight (1964) that gas bubbles may migrate due to the vapor transport of surrounding material across the bubble under influence of the temperature gradient. This happens in case when the gas (air) inside the bubble coexists with sufficient amount of vapor of the surrounding liquid. The mechanism of such migration is based on the fact that the vapor pressure p and vapor concentration c are sensitive to the temperature as given by:

$$p = p_0 e^{-\frac{l}{kT}} \tag{38}$$

and:

$$c = \frac{p_0}{kT} e^{-\frac{l}{kT}} \tag{39}$$

Here p_0 is the pressure constant for the vapor, l is the latent heat per atom, T is the average temperature in the bubble and k is the Boltzmann constant: $1.380649\ \ 10^{-23}$ J/K.

The flow of vapor atoms from the hot to the cold part of the bubble surface due to the vapor concentration difference gives rise to bubble migration velocity estimated in Speight (1964) as $u_B = ARdT/dx$. A is defined as follows:

$$A = \frac{1}{6\pi\gamma\sigma^2}\sqrt{\frac{8kT}{\pi m}}\frac{l}{T}\frac{p_0\Omega}{kT}e^{-\frac{l}{kT}} \tag{40}$$

Here R is the radius of the bubble, dT/dx is the temperature gradient, γ is the surface tension, σ is the diameter of the vapor atom, m is the mass of the vapor atom in and Ω is the volume of the vapor atom.

The following reasonable values of the above mentioned parameters have been set (mainly corresponding to water at room temperature, $25°C$):

$p_0 = e^{20.386}101325/760$ Pa
$l = (43.99$ kJ/mol$)/N_A = 43990/(6.022141\ \ 10^{23})$ J
$T = 298$ K
$\gamma = 71.97\ \ 10^{-3}$ N/m
$\sigma = 151.50\ \ 10^{-12}$ m

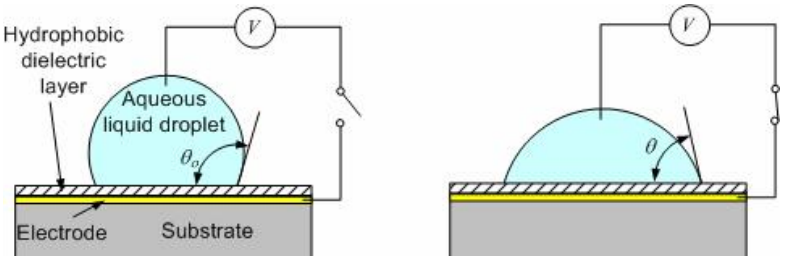

Figure 12: The droplet under the influence of electrowetting effect. Voltage applied to the electrode underneath the droplet leads to the reduction of the contact angle. Figure from Zhao & Cho (2007).

$m = 2.99151\ \ 10^{-26}$ kg
$\Omega = 4\pi\sigma^3/24$

Constant A in equation 40 can be estimated then as $3.820\ \ 10^{-6}$ m/s/K. This means that for example to reach the bubble velocity u_B of 10 μm/s it is required to apply a temperature difference to the opposite ends of the bubble of $u_B/A = 2.6$K. This requires enormous temperature gradients across the micrometer size bubbles, which makes this migration mechanism not practical.

7.3 Bubble velocity due to the electrostatic force

In present chapter we will estimate the electrostatic force acting on the air bubble embedded in water. According to L.D. *et al.* (1982) a spherical cavity of radius R in a surrounding dielectric with dielectric constant ε possesses an electric dipole moment p_E under influence of electric field Z:

$$p_E = 4\pi\varepsilon_0 \frac{1-\varepsilon}{1+2\varepsilon} R^3 Z \tag{41}$$

Here ε_0 is vacuum permittivity, $8.854\ \ 10^{-12}$ C/V/m.

This electric dipole moment induced by an impurity in a dielectric medium will experience a force $p_E dZ/dx$ due to the gradient of the electric field Z in space. So the force trying to move the bubble can be written as:

$$F = 3\frac{dZ}{dx} Z\varepsilon_0 \frac{1-\varepsilon}{1+3\varepsilon} V \tag{42}$$

V is the volume of the bubble, $V = 4\pi R^3/3$.

By choosing the values of the water dielectric constant $\varepsilon = 80$, radius of the bubble $R = 100\mu$m and quite optimistic values of electric field $Z = 100$ V/mm and its gradient $dZ/dx = 1$ V/mm/mm we get the value of the force in equation 42 of $5.46\ \ 10^{-12}$ N.

By using the Stokes law this force can be converted in effective bubble velocity u_B as follows: $u_B = F/(6\pi\eta R)$. By using the viscosity of water $\eta = 0.001$ Pa s it is apparent that $u_B = 2.9\mu$m/s, which is rather low. It is also visible from equation 42 that the bubble velocity decreases with the decreasing bubble radius as $\propto R^2$.

7.4 Electrowetting effect on bubbles

It is known from Zhao & Cho (2007) that electrowetting effect (see Mugele & Baret (2005)), which can be used to manipulate droplets (e.g. make the droplet spread over the surface by applying electric potential), can be used as well to influence bubbles.

The electrowetting effect is based on the dependence of the surface tension coefficients and the contact angles on the applied electric field (potential). The droplet under the influence of electricowetting effect is shown in figure 12.

This effect can be used to try to detach the bubble from the surface instead of spreading the droplet over the surface (see figure 13). Work (e.g. Zhao & Cho (2007)) shows that applying moderate voltages (50 - 90 V)

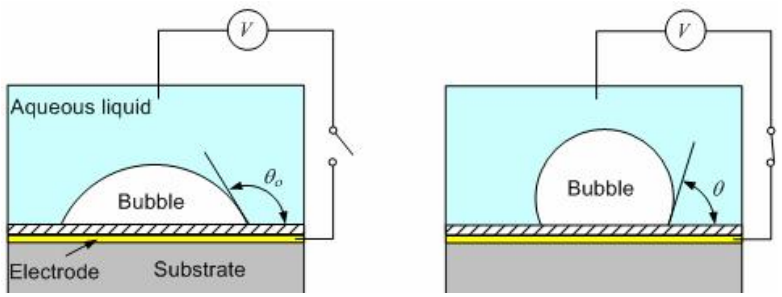

Figure 13: The bubble under the influence of electrowetting effect. Voltage applied to the electrode underneath the bubble leads to the reduction of the contact angle (from the liquid side). Figure from Zhao & Cho (2007).

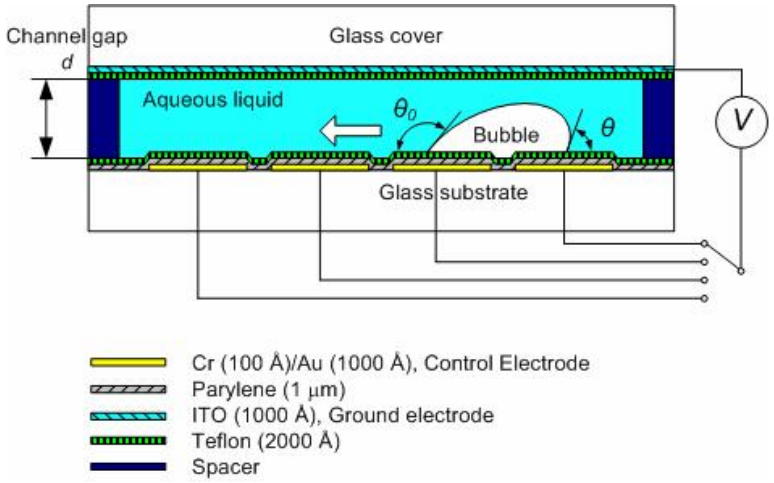

Figure 14: The illustration of the transport of the bubble by applying the voltage in sequence to the electrodes underneath the bubble. Figure from Zhao & Cho (2007).

to the electrode positioned under the dielectric surface on which the bubble is placed can result in reduction of the contact angle (from the liquid side) from 117° to 73°. Such manipulation can make the flushing of the bubble easier by increasing of the effect of the ink flow on the bubble.

Figure 14 from Zhao & Cho (2007) shows how the bubble can be transported in desired direction by applying voltage to a number of electrodes in sequence.

8 Conclusions & recommendations

The removal of a bubble from a corner has been investigated. When the bubble is not attached to the wall, but it is near the corner, the normal flushing operation should be sufficient to remove the bubble. The flow pattern that results from the flushing was calculated. The velocity close to the corner is still significant. The drag force on the bubble has been estimated.

In order to determine whether the viscous drag is sufficient to remove the bubble from the corner, the retaining force has been calculated by an analysis of the surface energy of a bubble in the corner and of a bubble in contact with a flat wall. For any finite contact angle, the energy of a bubble is lower in the corner, which gives rise to a retaining force. This retaining force is large enough to withstand the drag that would arise if the liquid were ejected with sonic (in air) speed from the nozzle, for a contact angle of 90°. For lower contact angles, the retaining force diminishes quickly. For a perfectly wetting surface, the capillary force on the bubble is zero.

For contact angles of 90° or more, the bubble cannot be removed by flushing. Preventing the bubble from

reaching the corner becomes very important in this case. Two effects that may be used to push the bubble away from the corner were examined. The first effect is thermal migration. Three kinds of thermal influence have been considered in this report. One of them is the Marangoni effect that moves the bubble due to the dependence of the surface tension on temperature. This is the dominant contribution to the thermal migration of the bubble. The other two thermal effects are thermal convection and transfer of the vapor across the bubble due to the temperature difference at the opposite sides of the bubble. These effects are both negligible. Of these three thermal effects, only the Marangoni effect is significant. The second effect is electromigration, where an electric field induces a force on the bubble. This force is too small to overcome secondary Bjerknes force, though electrowetting may be sufficient to reduce the retaining force enough to enable flushing.

Since bubbles can only be removed when the contact angle is small (hydrophyllic), controlling the wetting properties in the channel is crucial. Thermal migration may be used to prevent the bubble from reaching the corner, so that less ink is needed to flush the bubble. To use this effect, the corner must be kept cool. If these efforts prove to be insufficient, electrowetting can be investigated to enable flushing the bubble.

References

M. Brinkmann & R. Blossey (2004). Blobs, channels and " cigars" : Morphologies of liquids at a step. *European Physical Journal E*, 14(1):79–98.

R. Jeurissen (2009). *Bubbles in inkjet printheads: analytical and numerical models.* Doctoral thesis, University Twente.

L. L.D., E. Lifshitz & L. Pitaevskii (1982). Electrodynamics of continuous media. *Course of Theoretical Physics.*

H. K. Moffatt (1964). Viscous and resistive eddies near a sharp corner. *Journal of Fluid Mechanics*, 18(01):1–18. URL `http://dx.doi.org/10.1017/S0022112064000015`.

F. Mugele & J. Baret (2005). Electrowetting: from basics to applications. *Journal of Physics: Condensed Matter*, 17:705–774.

M. Prakash, D. Quéré & J. Bush (2008). Surface tension transport of prey by feeding shorebirds: The capillary ratchet. *Science*, 320(2878):931–934.

M. Speight (1964). The migration of gas bubbles in material subject to a temperature gradient. *Journal of Nuclear Materials*, 13(2):207–209.

N. Young, J. Goldstein & M. Block (1959). The motion of bubbles in a vertical temperature gradient. *Journal of Fluid Mechanics*, 6(03):350–356.

Y. Zhao & S. Cho (2007). Micro air bubble manipulation by electrowetting on dielectric (ewod): transporting, splitting, merging and eliminating of bubbles. *Lab on a CHip*, 7:273–280.